OCENA KAKOVOSTI VODE V ZBIRALNIKU DAU TIENG NA PODLAGI STANDARDNIH KRITERIJEV V KOMBINACIJI Z DALJINSKIM ZAZNAVANJEM SLIK

ASSESSMENT OF DAU TIENG RESERVOIR WATER QUALITY USING STANDARD CRITERIA COMBINED WITH REMOTELY SENSED IMAGES

Van Tran Thi, Bao Ha Duong Xuan, My Nguyen Thi, Thong Nguyen Hoang, Phuong Dinh Thi Kim, Truong Nguyen Nhut, Duong Pham Thuy, Trinh Ha Bao Van

UDK: 528.8:556.155(597)
Klasifikacija prispevka po COBISS.SI: 1.01
Prispelo: 20. 3. 2023
Sprejeto: 2. 8. 2023

DOI: 10.15292/geodetski-vestnik.2023.03.343-362
SCIENTIFIC ARTICLES
Received: 20. 3. 2023
Accepted: 2. 8. 2023

IZVLEČEK

Kakovost vode (WQ) je skrb vseh, zato je treba sprejeti sanacijske ukrepe za zaščito človeških življenj. V tem prispevku je predstavljena ocena kakovosti površinskih voda na podlagi indeksa kakovosti vode (WQI) po vietnamskem standardu QCVN 08-MT:2015/BTNMT v kombinaciji s satelitskimi podatki za zbiralnik Dau Tieng. Metoda izvajanja temelji na korelaciji vseh kazalnikov kakovosti vode s spektralnimi značilnostmi satelitskih posnetkov za oblikovanje regresijske funkcije, ki simulira prostorsko porazdelitev celotnega rezervoarja. Uporabljeni so bili satelitski posnetki Sentinel-2A z odsevnimi pasovi v vidnem in bližnjem infrardečem (NIR) spektralnem območju. Regresijske funkcije so pokazale, da je korelacija kazalnikov WQ povezana s posameznimi pasovi, razmerja med pasovi pa vključujejo modre in NIR, rdeče/modre, zelene/modre ter NIR/modre pasove. Rezultati simulacije prostorske porazdelitve WQI so pokazali, da je voda v rezervoarju Dau Tieng večinoma onesnažena, pri čemer je indeks WQI v razponu od 0 do 50. Namakalni sistem Dau Tieng ima pomembno vlogo v sistemu distribucije vode za provinco Tay Ninh in pomembno južno gospodarsko regijo. Zato je treba pred njegovo morebitno uporabo za oskrbo gospodinjstev z vodo sprejeti ustrezne ukrepe za čiščenje.

ABSTRACT

Water quality (WQ) pollution is a matter of concern to everyone, and it is necessary to take remedial measures to protect human life. This paper presents the assessment of surface WQ through the Water Quality Index (WQI) followed by the Vietnam Standard QCVN 08-MT:2015/BTNMT combined with satellite data for the Dau Tieng reservoir. The implementation method is based on the correlation of each WQ indicator with the spectral features of satellite images to build a regression function, simulating the spatial distribution of the entire reservoir. The Sentinel-2A satellite images were used with reflective bands in the visible and near-infrared (NIR) spectrum region. The regression functions showed that the correlation of the WQ indicators was related to single bands, and the band ratios include blue and NIR, red/blue, green/blue, and NIR/blue bands. Simulation results of the WQI spatial distribution expressed that the WQ of the Dau Tieng reservoir was in a polluted state at the level of WQI fluctuation in the range of 0–50 for the most part. Dau Tieng irrigation system plays a vital role in the water distribution system for Tay Ninh province and the southern key economic region. Therefore, appropriate treatment measures should be taken if it needs to be used for domestic water supply purposes.

KLJUČNE BESEDE

korelacija, regresija, sprektralni pas, kvaliteta vode, WQI

KEY WORDS

correlation, regression, spectral band, water quality, WQI

1 INTRODUCTION

Surface water quality (WQ) is one of the primary concerns for policymakers and environmental managers in both urbanized and agricultural areas. Both natural (discharge, rainfall, soil erosion, and physiological characteristics of the basin) and artificial factors (urbanization, industrial and agricultural activities, etc.) can affect the surface WQ. WQ is an important indicator that relates to all aspects of ecosystems and human life, such as public health, food production, economic activity, and biodiversity. From a management perspective, WQ is defined by its end-use needs. For the purpose of using water for drinking and habitat for aquatic plants and animals, the purity of water is often required at a higher level than for other purposes, such as meeting the needs of hydroelectricity and irrigation. Therefore, in a broad sense, WQ includes the physical, chemical, and biological factors necessary to meet user needs (WHO, 2011).

The science of remote sensing was born because the ground lacked much information, because humans could not go to the place and observe all over the region. This characteristic of the electromagnetic spectrum combined with ground observation points helps people simulate and speculate in the whole region how things are going through the pixel unit. Despite spatial resolution limitations, remote sensing is a good aid for seeing things according to the spatial distribution of the object's electromagnetic spectrum, and each pixel has a spectral value representing a type of terrestrial entity. A satellite image is an array of contiguous pixels, so when the satellite flies for an area, it can see the characteristics of the whole area based on all these actual pixels. We can simulate the whole region through the regression function between the measured value at the monitoring points on the ground and the spectral value of the satellite image pixels to which the monitoring point belongs. Specifically, the number of monitoring points is equivalent to a known number of pixels. From these known pixels, the regression function with the independent variable X being the spectral value of the entire satellite image makes it possible to speculate for the remaining pixels in the whole region. This is an interpolation algorithm based on the actual spectral characteristics of the entity in the whole region, so it can accept the number of ground samples within the allowable limits.

Meanwhile, for other sciences to be able to map a spatial distribution for the interested object in a region, it requires much sampling, covering most of the area to be able to interpolate for unknown points in the whole region. This is not feasible because it costs a lot of money and manpower. Especially in an area that wants to know the happenings simultaneously, it is impossible to have enough personnel to take samples simultaneously. Meanwhile, the satellite captures 1 image at a time to tell us everything that happens right on this moment. When we want to perform the correlation problem between the ground and the spectrum of satellite images, the monitoring points must be sampled at the same time. If sampling is taken at different days that are far from the satellite-acquired date, the spectral value of the one-day satellite image pixel will be difficult to correlate with the ground sample, especially for volatile objects such as water or air, or there is a possibility of false correlation that makes us misinterpret the accuracy of the model. Here we want to emphasize the Simultaneity: Simultaneously take samples at the same time the satellite takes pictures on the sampled area, so that the electromagnetic spectrum shown on the image pixel is a true representation of that sample characteristic.

Applications of remote sensing techniques have provided insight into the study of water resources in the context of rapid industrial development and intense urbanization. Since the 1970s, scientists have used satellites to detect optical spectra of components present in surface water (Ekstrand, 1992; O'Reilly et al., 1998). Since then, satellite models have become an attractive alternative to field monitoring methods. Remote sensing techniques provide regular, generalized coverage over large areas (Park & Ruddick, 2007). At a relatively low cost, remote sensing models can be developed to estimate the WQ distribution over entire water bodies, allowing monitoring and estimating contaminant concentrations in inaccessible areas. The Landsat satellite has had a relatively long operating time since the 1970s, so many studies have used Landsat sensor lines for WQ monitoring research and fluctuations over time. The research evaluates the relationship of spectral values on satellite images with chlorophyll-a parameters through a regression analysis algorithm (Alparslan et al., 2007; Guan, 2009; Al-Bahrani et al., 2012). Karakaya & Evrendilek (2011) applied Landsat 7 Enhanced Thematic Mapper Plus (ETM+) data to measure the concentration of nitrite nitrogen (NO_2-N) and nitrate nitrogen (NO_3-N) using best-fit multiple linear regression (MLR) models as a function of Landsat 7 ETM+ and ground data in Mersin Bay, Turkey. The studies of Phi et al. (2014), Fayma & Mili (2016), and Phuong et al. (2017) used Landsat 8 OLI satellite data to calculate more WQ parameters, including pH, chemical oxygen demand (COD), dissolved oxygen (DO), alkalinity, hardness, chloride, TDS, total suspended solids (TSS), turbidity, conductivity, and phosphate. In 2018, Prosper et al. conducted a comparative study of Landsat 8 and Sentinel-2 satellites in WQ mapping for two parameters, chlorophyll a and turbidity at Vaal dam. The results show that the Sentinel-2 image produces better results thanks to the higher resolution. Other studies use Sentinel-2 satellite images to determine the relationship with WQ parameters (WQP) (Ha et al., 2016; Karaoui et al., 2019; Sakuno et al., 2019). Ha et al. (2021) conducted multiple linear regressions of seven WQPs, including BOD, COD, NH_4, PO_4, TSS, pH, and Coliform, with surface water pixel spectral values from Sentinel-2 images. The results showed that there was a regressive correlation between measured data and image spectral values, and the simulation also fitted well with the data with an acceptable error. Most of these studies show that the WQPs are related to the image bands in the visible to NIR spectral range.

The water quality index (WQI) is calculated from the observed WQ indicators and used to describe the WQ quantitatively (VEA, 2011). WQI was first proposed and applied in the US in 1965-1970. After that, due to its many advantages, WQI was quickly accepted and applied in many countries worldwide, such as Canada, Argentina, the UK, Mexico, India, Thailand, and Zimbabwe. To assess the WQ and the level of water pollution, it is possible to rely on several essential criteria and limit regulations of each indicator following a country's Law on Environmental Protection or international standards specified for each type of water used for different purposes. In Vietnam, WQI was applied by researchers in the 1990s. In July 2011, the Vietnam Environment Administration (VEA), Ministry of Natural Resources and Environment issued Decision No. 879/QD-TCMT on issuing a manual for calculating the Vietnam Water Quality Index (VN_WQI) from national WQ monitoring data.

Our study assesses WQ based on VN_WQI (commonly called WQI in this study) combined with satellite data, used to quantitatively describe the WQ and the usability of that water source. The 8 parameters used to evaluate WQ are pH, DO, TSS, COD, BOD, N-NH_4, P-PO_4, and Coliform.

2 DATA AND METHOD

2.1 Study Area

Dau Tieng Reservoir is the focal work built upstream of Saigon River, at Dau Tieng junction in Dau Tieng district, Binh Duong province, located in the south of Vietnam, stretching from 11°12' to 12°00' North latitude and from 116°10' to 116°30' East longitude, about 100 km from Ho Chi Minh City along the inter-provincial road (Figure 1). Dau Tieng Reservoir has a basin area of 2,700 km^2, located in the territory of 03 provinces of Tay Ninh, Binh Duong, and Binh Phuoc, with a storage capacity of more than 1.58 billion m^3 of water and a surface area of 270 km^2. Located upstream of the Saigon River, the Dau Tieng Reservoir plays a vital role in storing fresh water supply, regulating the hydraulic environment, regulating floods and salinity downstream, aquaculture, tourism, and ecological conservation, related to the lives of millions of people in the provinces of Tay Ninh, Binh Duong, Binh Phuoc and Ho Chi Minh City (DT-PH IEIC, 2019) (Figure 1). The reservoir basin lies on a transitional terrain. The upstream area in the east is a low hill in the shape of a basin gradually sloping towards the two main rivers (Saigon River and Ba Hao River). The topographic slope is northeast-southwest in the direction of the area's main prevailing monsoon; besides, this is not the direction to catch the wind and bring rain, except for the upstream area controlled by the Tong Le Chan branch. The altitude above sea level is 25–27 m. The upstream part of the basin belongs to Cambodia, with an elevation of 50–100 m above sea level. The reservoir bed area has an elevation of 5–15 m, sometimes < 5 m. Basin geology is formed by Quaternary sediments, consisting of sedimentary materials ranging from clay to gravel, and Neogene Quaternary deposits made up of sedimentary rocks and mud (DT-PH IEIC, 2019).

Dau Tieng Reservoir is located in the Saigon River basin and is influenced by the basin climate with tropical monsoon characteristics. The climate is divided into 2 distinct seasons: The rainy season starts from May to November; The prevailing wind is the southwest monsoon with an average speed of about 1.6–2.1 m/s and causes heavy rain. The dry season starts from December to April; The prevailing wind in this period is the northeast monsoon with an average speed of about 1.8–2.2 m/s; The wind carries dry air and creates a dry season, with rainfall accounting for only 10–15% of annual rainfall. The average annual rainfall across the basin is about 1,810 mm. The heaviest rainfall over 300mm usually occurs in September and October. Dau Tieng Reservoir gets water from rivers and streams, including Nuoc Duc and Krai flowing from Cambodia to form the Tha La River in the west of the reservoir; Ngo, Xa Cat, and Lap streams flowing into the reservoir from Binh Phuoc province in the east. The Dau Tieng basin has two distinct seasons. The flood season starts in September and lasts until the end of December. The dry season lasts from 8–9 months of the year. 70–80% of the total flow in the year is concentrated in 3–5 months of the rainy season. Only 20–30% of the flow is concentrated during the dry season. The annual inflow is 20–25 l/s-km^2. The amount of inflow is mainly upstream during the flood season. The reservoir is also affected by groundwater inflow, which is less than surface water (DT-PH IEIC, 2019).

The bed of Dau Tieng Reservoir is divided into two areas: a flooded area and a semi-submerged area. According to the operation process, the lake has a water level varies from 17–24.4 m. The reservoir accumulates water from the beginning of July to the end of November, then drains for the rest of the time, revealing the semi-submerged area. People living around the reservoir have taken advantage of favorable conditions in the semi-flooded area to cultivate agriculture and raise cattle and poultry. In

the flooded area, the upper reservoir has two tributaries, the East and West. Due to the characteristics of the eastern tributary, which has a large discharge and a much higher upstream slope than that of the western tributary, the amount of alluvium deposited into the reservoir is quite large. Therefore, sand mining activities occur strongly here (My, 2019).

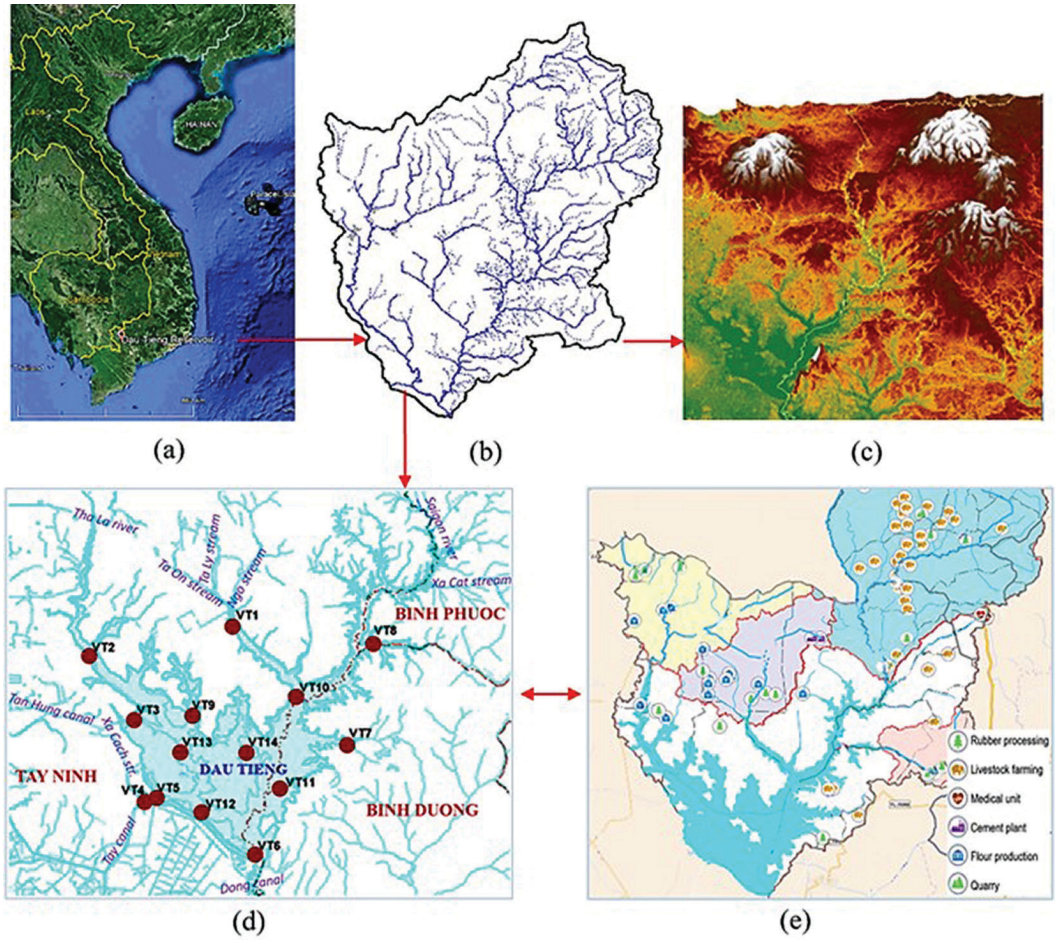

Figure 1: (a) Shape of Vietnam on Google Earth, (b) Dau Tieng Reservoir basin, (c) 3D topographic simulation of Dau Tieng Reservoir basin, (d) Shape of Dau Tieng Reservoir and location of monitoring points, (e) Production activities in Dau Tieng reservoir basin refer from DT-PH IEIC (https://bwe.com.vn/hodautieng/)

2.2 Data

Ground monitoring data are water samples observed at 14 points on the reservoir collected on March 2, 2019, from Dau Tieng - Phuoc Hoa Irrigation Engineering Integrated Company (DT-PH IEIC), responsible for managing the Dau Tieng Reservoir. The location of water sample monitoring points is mainly established at particular points related to production activities or farming to monitor the water quality discharged into the reservoir. Samples were collected, processed, and analyzed according to current Vietnamese standards. The parameters used in the study include pH, COD, BOD,

TSS, DO, N-NH_4, P-PO_4, and Coliform. Surface water analysis results are compared with QCVN 08-MT:2015/BTNMT – National technical regulation on surface WQ. Table 1 and Figure 1 show the sampling location and water quality analysis results. In addition, the field trip from March 25, 2021, to March 29, 2021, was conducted to survey the discharge status of production units on the banks of the Dau Tieng reservoir.

Table 1: Sampling location of monitoring points on Dau Tieng reservoir and results of water quality analysis on March 2, 2019 (DT-PH IEIC, 2019)

Sampling area characteristics	Sample code	pH	DO (mg/l)	COD (mg/l)	BOD (mg/l)	TSS (mg/l)	N-NH4 (mg/l)	P-PO4 (mg/l)	Coliform (MPN/ 100ml)
-Ngo stream (rubber and flour processing factory)	VT1	5.8	3.05	16	6.0	36	0.71	0.35	280
-Tha La River (rubber and flour processing factory)	VT2	10.4	3.45	34	7.5	34	2.31	0.97	260
-Culvert 3 (TanHung canal)	VT3	7.5	3.35	29	6.6	30	2.21	0.55	200
-Xa Cach stream (noodle factory)	VT4	8.3	3.35	32	6.8	34	0.81	0.65	240
-Culvert 2 (Tay Canal)	VT5	9.7	3.45	32	7.1	32	1.81	0.75	240
-Culvert 1 (Dong Canal)	VT6	9.2	3.25	28	7.2	34	2.51	0.8	210
-Phuoc Hoa Canal (livestock farming)	VT7	7.1	3.05	12	6.2	24	0.11	0.25	240
-Tributary of Saigon River (rubber processing factory)	VT8	6. 9	2.85	10	6.1	31	0.01	0.15	210
-Near Culvert 3	VT9	7.6	3.15	22	6.2	30	1.31	0.47	205
-Near the tributary of Saigon River (Tong Le Chan pig farm)	VT10	7.2	3.05	17	6.4	28.5	1.01	0.52	190
-Near Phuoc Hoa Canal (rubber processing factory)	VT11	8.8	3.25	24	6.8	29	2.31	0.67	220
-Near Culvert 1	VT12	9.1	3.15	30	7.1	31	1.51	0.63	210
-Near Culvert 2	VT13	8.6	3.35	27	6.5	20	2.11	0.54	220
-In the middle of the reservoir near the island of Nhim (cultivation and farming)	VT14	7.8	3.25	32	7.0	28	2.11	0.70	190

The satellite image data used is the Sentinel-2A image. Sentinel-2A satellite was launched on June 23, 2015, carrying Multi-Spectral Instrument (MSI) with a high revisit time (10 days at the equator). Sentinel-2 carries an optical instrument payload that samples 13 spectral bands: four bands at 10 m (bands 2, 3, 4, and 8), six bands at 20 m (bands 5, 6, 7, 8a, 11, and 12) and three bands at 60 m (band 1, 9, and 10) spatial resolution. The orbital swath width is 290 km (ESA, 2015). We use high-resolution optical satellite images Sentinel-2A acquired on March 2, 2019, coinciding with the time of collecting water samples observed at 14 locations, to evaluate the spatial distribution of the surface WQ parameters. 14 sampling points in our study were carefully selected within one day of sampling, which is coincided to the date of the satellite image acquired to ensure the lowest differences. And if we have to take samples of many days, we have to ensure that enough satellite images of the days coincide with the sampling date. Meanwhile, the repetition period for one shot in an area depends on the type of satellite. With optical properties influenced by cloud cover, not all images taken are visible

to the ground to be used. Here, because the lake size is not very large, we have focused on choosing the maximum number of samples in one day of observation that matches the date of the best-selected satellite image to perform regression analysis and simulation. The spectral reflectance of water extends in the visible and partly in the NIR wave region, strongest in the blue and a little in the green wave region (Van et al., 2017). Therefore, the Sentinel-2A image consists of 13 image bands, in which we only use the bands in the visible and near-infrared bands (bands 2, 3, 4, 8) with a spatial resolution of 10m. In addition, two satellite images acquired on January 6, 2019, and October 28, 2019, are used to monitor WQ at other times of the year.

2.3 Method

2.3.1 Methods to assess surface water quality

Our calculation is based on (1) QCVN 08-MT: 2015/BTNMT - National Technical Regulation on Surface WQ of the Ministry of Natural Resources and Environment; (2) Decision 879/QD-TCMT dated July 1, 2011, of the Vietnam Environment Administration, issued a manual for calculating WQI from environmental monitoring data of continental surface water. The WQ indicators used for the study were pH, DO, COD, BOD, TSS, N-NH_4, P-PO_4, and Coliform.

The QCVN 08-MT:2015/BTNMT is a National technical regulation stipulating the classification of surface water sources into four groups (A1, A2, B1, and B2) for assessing and controlling water quality for the different purposes of utilization (Table 2). Each indicator has a limit value determined by each group (Table 3).

To calculate WQI, it is necessary to determine the WQI_{SI} value for each indicator according to Eq. (1) to consider the effect of each indicator on WQ (VEA, 2011).

$$WQI_{SI} = \frac{q_i - q_{i+1}}{BP_{i+1} - BP_i}\left(BP_{i+1} - C_p\right) + q_{i+1} \tag{1}$$

In which, SI is the symbol that represents 8 WQ indicators, so WQI_{SI} is the calculated water quality index for each indicator; BP_i is the lower limit concentration of the monitoring parameter value corresponding to level i; BP_{i+1} is the upper limit concentration of the observed parameter value corresponding to the level i+1; q_i is the WQI value at level i given in the table corresponding to the BP_i value; q_{i+1} is the WQI value at i+1 given in the table corresponding to the BP_{i+1} value; C_p is the value of the observed indicator to be included in the calculation. The reference values are presented in Tables 4a and 4b.

The total WQI is determined using Eq. (2) to assess the reservoir WQ (VEA, 2011).

$$WQI = \frac{WQI_{pH}}{100}\left[\frac{1}{5}\sum_{a=1}^{5} WQI_a \times \frac{1}{2}\sum_{b=1}^{2} WQI_b \times WQI_c\right]^{1/3} \tag{2}$$

In which WQI_a is the calculated WQI value for 05 indicators: DO, BOD, COD, N-NH_4, P-PO_4; WQI_b is the calculated WQI value for the TSS indicator; WQI_c is the calculated WQI value for the total Coliform indicator; WQI_{pH} is the calculated WQI value for the pH indicator. Finally, the WQI value is compared with Table 5 to evaluate the WQ levels.

Table 2: Classification of surface water quality by QCVN 08-MT:2015/BTNMT (MONRE, 2015)

Group	Description
A1	the WQ is suitable for use for domestic water supply (after applying standard treatment), aquatic flora and fauna conservation, and other purposes such as grade A2, B1, and B2
A2	the WQ is suitable for use for domestic water supply purposes but must apply appropriate treatment technology or use purposes such as B1 and B2
B1	the WQ is suitable for use for irrigation or other uses with similar water quality requirements or uses as class B2
B2	the WQ is suitable for use for navigation and other purposes with low-quality water requirements

Table 3: Limit values of surface water quality by classification groups of QCVN 08-MT:2015/BTNMT (MONRE, 2015)

Indicator	Unit	Limit values			
		A1	**A2**	**B1**	**B2**
pH	-	6–8.5	6–8.5	5.5–9	5.5–9
DO	mg/L	≥ 6	≥ 5	≥ 4	≥ 2
COD	mg/L	10	15	30	50
BOD	mg/L	4	6	15	25
TSS	mg/L	20	30	50	100
N-NH_4^+	mg/L	0.3	0.3	0.9	0.9
PO_4^{3-}	mg/L	0.1	0.2	0.3	0.5
Coliform	MPN/100 ml	2,500	5,000	7,500	10,000

Table 4a: Regulation of qi, BPi values for the indicators participating in the calculation WQI (except pH) (MONRE, 2015)

i	qi	DO	COD	BOD	N-NH_4	P-PO_4	TSS	Coliform	Indicator colour
		mg/L						MPN/100 mL	
1	**100**	≥ 6	≤ 10	≤ 4	≤ 0.1	≤ 0.1	≤ 20	≤ 2500	Blue
2	**75**	6–5	10–15	4–6	0.1–0.2	0.1–0.2	20–30	2500 – 5000	Green
3	**50**	5–4	15–30	6–15	0.2–0.5	0.2–0.3	30–50	5000 –7500	Yellow
4	**25**	4–2	30–50	15–25	0.5–1	0.3–0.5	50–100	7500–10000	Orange
5	**1**	< 2	> 50	> 25	> 1	> 0.5	> 100	>10000	Red

Table 4b: Regulation of qi, BPi values for pH indicators (MONRE, 2015)

i	**1**	**2**	**3**	**4**	**5**	**6**
BP_i	≤5.5	5.5	6	8.5	9	≥9
q_i	1	50	100	100	50	1
Indicator colour	Red	Yellow	Blue	Blue	Yellow	Red

Table 5: WQI Classification levels and suitability for use according to Decision 879/QD-TCMT (VEA, 2011)

i	WQI	WQ	Suitable for the intended use	Indicator colour
1	**91 – 100**	Excellent	Good use for domestic water supply purposes	Blue
2	**76 – 90**	Good	Use for domestic water supply purposes but need appropriate treatment measures	Green
3	**51 – 75**	Moderate	Use for irrigation and other equivalent purposes	Yellow
4	**26 – 50**	Poor	Use for navigation and other equivalent purposes	Orange
5	**0 – 25**	Very Poor	Water is heavily polluted and needs future treatment measures	Red

2.3.2 Remote sensing method

The WQ assessment from ground observation data only shows the results at the sampling point. It limits the ability to track WQ throughout the lake (Ritchie et al., 2003). A satellite image presents the current situation over space in pixels. Each pixel represents the current state at the observation location. Therefore, satellite images can assess the phenomenon of the whole lake.

The spectral reflectance of water extends in the visible and partly in the NIR wave region, strongest in the blue and a little in the green wave region (Van et al., 2017). Therefore, every single band investigates the correlation between 8 WQ indicators and the spectral value in the blue, green, red, and NIR wave regions. Besides, the spectrum band transformations according to the band ratio also are considered to expand the observed variables. Band ratios are performed on these 4 image bands with the permutation of each band pair: blue/green, blue/red, blue/NIR, green/blue, green/red, green/NIR, red/blue, red/green, red/NIR, NIR/blue, NIR/red, NIR/green. From this correlation result, regression functions are built to simulate the spatial distribution of the indicators on the reservoir based on satellite images. Then WQI calculation steps are performed according to Eq. (1) and (2) based on 8 WQ indicators calculated on each image pixel to determine the spatial distribution of water pollution.

In addition, to track the difference in WQ lakes over time, we performed relative radiometric normalization (RRN) for the different images. Satellites that receive reflected signals from an object on the earth surface always have certain deviations from their true reflectance values (absolute reflectivity) due to different atmospheric conditions and lighting from different recorded dates (Vermote et al., 1997; Mateos et al., 2010). Radiometric normalization is intended to return these values to actual values. To compare two images with each other, one can use the relative or absolute normalization method, which is reducing the spectral reflectance characteristics obtained on the two images to one. The absolute normalization method is challenging due to the lack of atmospheric information associated with the image. RRN does not require ground measurements of the atmosphere at the time of acquisition and is not necessary to know the absolute reflectivity of images (Canty, 2010). It is assumed that the relationship between the radiance obtained by the sensors on two different dates in the same area can be approximated by a linear function. Then, when implementing the RRN, the conversion equation between the two images has the form (Mateos et al., 2010):

$$u_k = a_k x_k + b_k \tag{3}$$

Where u_k is the pixel band k value on the first image, called the reference image; x_k is the pixel band k value on the second image, called the subject image; a_k, b_k are coefficients. Coefficients a_k and b_k are calculated based on regression analysis of unchanged objects on two images. These immutable objects are often chosen as time-invariant points.

Accordingly, an image is used as a "reference image." The other image is a "subject image," meaning that the image is corrected for atmospheric, geometrical, lighting, and environmental conditions according to the "reference" image. We used satellite images acquired on March 2, 2019, as a reference image to normalize relative radiation for two satellite images acquired on January 6, 2019, and October 28, 2019.

To extract information from satellite images, it is necessary first to perform image preprocessing steps, including radiation correction and geometry correction. Radiation correction was used to convert the

digital number value of a pixel to a spectral irradiance value with units of $W.m^{-2}.ster^{-1}.\mu m^{-1}$. Next, a geometric correction step was carried out to eliminate the geometrical errors caused during the image acquisition process and bring the images to the local coordinate system of Vietnam, VN-2000. Images were geometrically corrected by map-based image manipulation.

2.3.3 Statistical method

Pearson correlation coefficient (r) is a statistical indicator that measures the correlation relationship between two variables, applied in this study with the dependent variable being the spectral value extracted from satellite images (y), and the independent variable being ground observation data (x) of the 8 WQ indicator for the 14 selected sites. The Pearson's correlation basic equation is defined as Eq. (4). Then, a linear regression analysis was conducted for all WQ indicators.

$$r = \frac{\sum_{i=1}^{n}(x_i - \overline{x})(y_i - \overline{y})}{\sqrt{\sum_{i=1}^{n}(x_i - \overline{x})^2 \sum_{i=1}^{n}(y_i - \overline{y})^2}} \tag{4}$$

When performing regression analysis, if the independent variables are strongly correlated, the problem of multicollinearity must be taken into account. Multicollinearity can lead to skewed or misleading results when we attempt to determine how well each independent variable can be used most effectively to predict or understand the dependent variable in a statistical model. The variance inflation factor (VIF) can detect and measure the amount of collinearity in a multiple regression model. The SPSS software package was employed for data treatment.

Our study aims to not perform predictive modeling, but build relationships between the spectral value from satellite images and the ground observation value using regression functions to simulate the status of spatial distribution of the interested object, including WQ indicators and WQI.

2.3.4 Validation

Observation samples include 14 locations over the reservoir. With 14-point ground data, we divided the data into 2 parts: training with 13 points, and testing with the remaining 1 point. We ran the regression model with 13 points and 1 point to test the model, to get Root Mean Square Error (RMSE) and R^2. Continue to run the regression model for the second time, with 13 points and 1 point (different from the first run) to get the second result. Similarly, with 14 points, the regression model will be run 14 times, resulting in 14 sets of RMSE and R^2 values. Finally, we selected 2 results with the smallest RMSE corresponding to 2 test points, VT6 and VT7. We used 12 samples to run the regression and 2 samples to control the error assessment according to each WQ indicator. The accuracy evaluation error is calculated from the mean deviation (bias) between the estimated values and the actual measured value according to Eq. (4).

$$\text{bias} = \frac{1}{N}\sum_{i=1}^{N}(T_S^e - T_S^m) \tag{4}$$

Where N is the number of samples taken to calculate the error; and T_S^e are T_S^m the value estimated from satellite images and actual measured data.

The total accuracy of the regression model is evaluated by the least squares method (Eq. (5)). The error is calculated based on the squared difference between the actual value (of the reference points) and the simulated value (in the regression model).

$$\mathrm{RMSE} = \sqrt{\frac{\sum_{i=1}^{n} (T_s^e - T_s^m)^2}{n}} \tag{5}$$

This Equation is also applied to the case of relative radiation normalization before and after normalization (Trung, 2015).

3 RESULTS AND DISCUSSION

3.1 Regression analysis and simulation of the spatial distribution of the WQ indicators

The 8 WQ indicators used for the study were shown above. How each indicator is considered affects the lake WQ. The regression equation is required to explain the relationship between the spectral radiance with ground monitoring data. The single band and the band ratio images were treated as independent variables in the simple linear regression model. We analyzed correlation to select variables with high correlation coefficients with R > 0.7 and p-value < 5%. Statistical results of high correlation coefficients of single bands and band ratios of WQ indicators are presented in Table 6. This table shows that each WQ indicator has at least 2 to 7 variables that meet the conditions and are selected for regression analysis. However, these correlated variables can autocorrelation in the case of multicollinearity. Therefore, we have implemented a stepwise regression method to detect multicollinearity by calculating the VIF index, then to remove falsely correlated variables. Next, we ran multiple regression equations simultaneously (Linear, Quadratic, Logarithmic, Cubic, Power, ...) for that variable to find the most suitable form of equation. After performing regression analysis, the most statistically significant variables were selected. From there, a regression equation for the WQ indicator with the most suitable variable was built, as presented in Table 7. We simulated the spatial distribution for each WQ indicator on the Dau Tieng reservoir from the built regression equations and presented it in Figure 2(2). Statistics for each WQ indicator from this simulation result are presented in Table 8.

Table 6: Single bands and band ratios with a high correlation coefficient with each WQ indicator

Indicator	Single bands, band ratios as Variable	Note
pH	Blue, Green, Red, Green/Blue, Red/Blue, Red/Green	R > 0.7 p-value <5%
COD	Blue, Green, Red, Green/Blue, Red/Blue, Red/Green	
BOD	Blue, Green, Red, Green/Blue, Red/Blue, Red/Green	
DO	Green, Red, Green/Blue, Red/Blue, Red/Green	
TSS	NIR, NIR/Blue	
N-NH_4	Blue, Green, Red, Green/Blue, Green/NIR, Red/Blue, Red/NIR	
P-PO_4	Blue, Green, Red, Green/Blue, Red/Blue, Red/Green	
Coliform	NIR, NIR/Blue	

Table 7: Regression equation determined for WQ indicator

Indicator	Regression equation	Pearson R	X variable	Simulation Results	Unit
pH	Y = 8.284X + 0.596	0.879	X = Red/Blue	5.8–10.4	mg/L
COD	Y = 50.20X - 20.599	0.900	X = Red/Blue	6.8–55.1	mg/L
BOD	Y = 4.7646X + 1.4428	0.843	X = Green/Blue	5.5–7.8	mg/L
DO	Y = 1.164X + 2.1647	0.879	X = Red/Blue	2.80–3.92	mg/L
TSS	Y = 14.677X + 23.393	0.865	X = NIR/Blue	28–70	mg/L
N-NH_4	Y = 0.003X - 4.122	0.855	X = Blue	0.01–2.57	mg/L
P-PO_4	Y = 2.306X - 1.953	0.927	X = Green/Blue	0.15–1.13	mg/L
Coliform	Y = 0.154X + 89.155	0.925	X = NIR	175–658	MPN/100 mL

From the location information of 14 monitoring points (Table 1), the figure of production activities in the Dau Tieng reservoir basin referring to DT-PH IEIC (https://bwe.com.vn/hodautieng/) (Figure 1e), and field information, we evaluate simulation results of WQ indicators on the Dau Tieng reservoir with the following characteristics (Table 7).

The pH index in the study area ranged from 5.8 to 10.4. In particular, a higher pH value (pH>7) indicates alkaline water, whereas a lower pH number (pH<7) indicates acidic water. Generally, the pH index in the Northwest and Southwest regions was higher than in the rest. Specifically, the Northwest region (upstream of the Tha La River tributary) had a pH >9 (shown in red). The eastern area (a tributary of Phuoc Hoa Canal) receives water from Phuoc Hoa Lake, so the pH index was more stable, ranging from 6 to 8.5 (shown by the blue colour). However, there was a clear difference in the position of the Phuoc Hoa Canal. The direction of the Saigon River tributary had a significantly different pH value, ranging from 5.5 to 6, due to cattle-raising activities of business households affecting water quality (according to observations from our field information). In the middle of the reservoir, the pH index ranged from 6.5 to 8, but the more downstream, the more the pH changed in a poor direction. Although raft farming in the Dau Tieng reservoir has been prevented, the neighboring areas still raised fish and discharged water directly into the lake. Besides, the production activities of noodle factories, rubber factories, pig farms, and sand mining activities directly affected WQ (DT-PH IEIC, 2019).

TSS concentrations ranged from 28 to 70 mg/L in classification levels of A2, B1 and B2 of QCVN 08-MT:2015/BTNMT. Upstream of Tha La and Saigon tributaries had TSS concentrations fluctuating within classification B1 because these areas had sand mining and livestock farming activities, which led to high concentrations of suspended matter in the water (DT-PH IEIC, 2019). In the middle of the reservoir, TSS concentration reached classification A2, suitable for the purpose of domestic water supply, but treatment measures were required. B2 class had pixels scattered throughout the reservoir and occupied an insignificant area of about 39,600 m^2.

COD concentrations ranged from 6.8 to 55.1 mg/L in classification levels of A1, A2, B1, B2, and exceeding level B2 of QCVN 08-MT:2015/BTNMT. Most areas on the Dau Tieng reservoir had COD concentrations reaching column B1. In the Northeastern area of the tributary of the Saigon River, the COD concentration was quite good, reaching the classification of A1 and A2. In contrast, the northwest of Tha La stream and the west of Xa Cach stream area near Culvert 2 of VT5 had relatively high COD concentrations, fluctuating within the B2. Water in the middle of the reservoir had COD concentrations in class B1, suitable for irrigation purposes.

BOD concentration spatially distributed was relatively stable, ranged from 5.5 to 7.8 mg/L, predominantly in class B1 for the whole reservoir, achieving a quality adequate for the purpose of irrigation and drainage. The upstream area of the Saigon River tributary had a lower BOD concentration, ranging in column A2, achieving a quality adequate for the purpose of the domestic water supply, but it needed to be treated.

$N\text{-}NH_4$ and $P\text{-}PO_4$ concentrations were within the alarming range, and these parameters had similar alarm points. The concentration of $N\text{-}NH_4$ ranged from 0.01 to 2.57 mg/L, and the concentration of $P\text{-}PO_4$ ranged from 0.15 to 1.13 mg/L. The upstream area of Tha La River tributary to the downstream Culvert 1 at VT12 had $N\text{-}NH_4$ <1 mg/L and $P\text{-}PO_4$ <0.5 mg/L exceeding column B2 of QCVN 08-MT:2015/BTNMT. This means that the water source was heavily polluted and needed to be treated in the future. In contrast, upstream of the Saigon tributary, the concentrations of $N\text{-}NH_4$ and $P\text{-}PO_4$ were lower (shown in blue and green). It shows that the status of ammonium and phosphate pollution in the study area was alarming, and it was necessary to improve water quality.

The spatial distribution of DO concentration was relatively stable, ranging from 2.80 to 3.92 mg/L, suitable for irrigation purposes. To use water for domestic purposes, it was necessary to take measures to minimize the impact of water pollution. The Coliform indicator had a relatively low concentration, ranging from 175–658 MPN/100mL, reaching the A1 level of QCVN 08-MT:2015/BTNMT.

Generally, the concentrations of WQ indicators at the study time differed according to spatial distribution. The concentration of three indicators, $N\text{-}NH_4$ and $P\text{-}PO_{4,}$ did not reach the specified limit, most exceeded the allowable limit (shown in red). In contrast, the Coliform, BOD, COD, and TSS indicators had quite good values for the purposes of domestic water supply, irrigation, and drainage. In particular, the pH distribution in the reservoir was quite diverse, with some areas showing heavy pollution and some showing good WQ, which was consistent with the actual status of the reservoir. The remaining indicator DO was valid for only irrigation purposes.

3.2 Water quality situation of Dau Tieng reservoir

The concentration description of each WQ indicator is meaningful only for that substance. The WQ of the lake is evaluated based on the sum of the concentrations of the WQ indicators (Eq.(2)), expressed by WQI used to describe the WQ and usability of that water source quantitatively and is represented by a scale (Table 5) (MONRE, 2015). The WQI simulation results illustrated in Figure 3(b) shows that water at the time of the study had a relatively straightforward spatial distribution of pollution. Notably, the downstream area at the discharge points (VT3, VT5, VT6) showed heavily polluted water sources (shown in red). The water in this area was heavily polluted due to the main business activities: noodle factories and large-scale cattle raising (>1000 pigs/herd). Wastewater from production and livestock activities was discharged directly into the reservoir. The downstream area is the place to distribute water from the reservoir to places where there is a need for use through the drainage canal system (DT-PH IEIC, 2019). If the pollution is not reduced, it affects people health by using water for domestic purposes.

The upstream area of the Tha La stream (to the left of the reservoir) receives water from three streams, including Ta Ly, Ta On, and Ngo streams. These streams received wastewater from noodle and rubber factories, and intense sand mining occurred in this area. According to statistics, about 4 sand mines were licensed to operate in the Tha La stream area, not to mention illegal sand mining activities. It led to the

water in this area being heavily polluted (shown in red). The water source was shown to be heavily polluted in the area where the Saigon River intersects with the reservoir bed (DT-PH IEIC, 2019). Large-scale and unsanitary livestock-raising activities (pig farms) led to contaminated wastewater being discharged into the reservoir. In addition, people living along the reservoir used water for daily life and directly discharged domestic wastes into the reservoir, leading to polluted reservoir water (DT-PH IEIC, 2019). The remaining areas, such as the Ngo stream upstream, the lake's northern half, and the Phuoc Hoa canal area, showed moderate WQ. The WQI ranged from 51 to 75, so water was used only for irrigation. Dau Tieng Reservoir plays a significant role in storing fresh water supply, regulating the hydraulic environment, regulating floods and salinity downstream, aquaculture, tourism, and ecological conservation, related to the lives of millions of people in the provinces of Tay Ninh, Binh Duong, Binh Phuoc, and Ho Chi Minh City. Therefore, it is necessary to manage and monitor the causes of reservoir water pollution to protect the quality of water sources and ensure the health of people and the living environment in general.

The research results were evaluated by validation to verify the calculation process. The evaluation was carried out by comparing calculation results and measures: (1) according to each WQ indicator; (2) according to WQI. For the first case, the 8 participating indicators in the WQ calculation had RMSE ranging from 0.06 to 5.66. The 5 indicators, pH, BOD, DO, P-PO_4, and N-NH_4, had error results below 1, ranging from 0.06 to 0.93. The remaining three indicators, COD, TSS, and Coliform, had relatively large error rates, including 2.83, 1.41, and 5.66. However, comparing with QCVN 08-MT:2015/BTNMT, it showed that the limit value of these 3 parameters was quite significant, specifically COD in the range of 10–50 mg/L, TSS in the range of 20–100 mg/L, and Coliform in the range 2500–10000 MPN/100mL (Table 4a). If the concentrations of indicators differ by ≤ 5 values, the threshold for WQ classification in QCVN 08-MT:2015/BTNMT remains unchanged. It showed that the error of 3 indicators, COD, TSS, and Coliform was acceptable.

In the case of error according to WQI simulated from satellite images, we performed a direct calculation based on ground observation data at 14 sampling locations and compared the quality level on a 5-point scale, as in Tables 4a and 4b (the results were presented in Figure 4). The comparison results showed similar WQI levels between the simulation and measurement data sets. Specifically, as shown in Figures 3b and 4, at observation points VT2, VT5, VT6, and VT12, the water source has the heaviest pollution in both data sets; Monitoring point VT11 has low WQI, reaching level Poor; while VT1, VT3, VT9, VT10, VT13, and VT14 have WQI reaching Moderate level. However, there are 3 observation positions with deviations between the 2 sets of simulated and measured data as follows: at the VT4 point, the measured WQI is Average, while the WQI simulation results from satellite images show the quality level as Poor; 2 observation points VT7 and VT8 have the actual measured WQ level as Good, while the results on the simulation image represent the Moderate level. This deviation can explain by 2 reasons as followings: (1) The built regression model also has certain errors when the correlation coefficient is considered mostly within 0.8-0.9 with p-value <5% (Table 7); (2) The spatial resolution of the satellite image also causes this limitation. Sentinel-2A image bands have a spatial resolution from 10–20m. In this study, we used bands with a spatial resolution of 10m (Table 6). It means that the spectral values of the objects are averaged in one pixel with a cell size of 10x10m. In contrast, the ground monitoring data is at only one sampling point (Phi et al., 2014; Van et al., 2017). Regarding the limitation of satellite image resolution, we orient future research with different resolution enhancement algorithms and search for higher-resolution image sources.

To understand more about the distribution of WQ in the whole Dau Tieng reservoir at other times, we further analyzed the images acquired on January 6, 2019, and October 28, 2019. Satellite images are acquired thanks to the radiating process of solar energy in space, so each time, the image is influenced by environmental and atmospheric conditions. The RRN allows the image to be changed according to the conditions of the reference image (Mateos et al., 2010). Therefore, two satellite images acquired on January 6, 2019, and October 28, 2019, have to be relatively normalized to radiation according to satellite images acquired on March 2, 2019, to apply WQ simulation regression models for all 2 times in 2019.

The analyzed results indicated that the appropriate model was related to bands 2, 3, 4, and 8 of the Sentinel-2A satellite image. Therefore, we performed RRN for these bands on the January and October images. 50 pairs of points extracted from each image were invariant or with tiny variations to determine relative normalization functions (RNF). X is the original image pixel, and Y is the normalized image pixel, as presented in Table 8. Based on the image of January 6, 2019, and the image of October 28, 2019, that have been transformed after this process, the corresponding single bands and band ratios were made to apply the regression function to simulate the spatial distribution of the WQ indicators and the WQI for Dau Tieng reservoir (Figures 2(1), 2(3) and 3(a), 3(c)).

Table 8: Defined relative normalization functions for Sentinel-2A images acquired on January 6, 2019, and October 28, 2019

Variables	RNF of 06/01/2019	RNF of 28/10/2019
Band 2	Y = 0,3381X + 924,76	Y = 0,3073X + 945,48
Band 3	Y = 0,3487X + 874,08	Y = 0,3055X + 923,89
Band 4	Y = 0,4606X + 713,72	Y = 0,2475X + 980,76
Band 8	Y = 0,2352X + 1936,7	Y = 0,3281X + 1642,3

Dau Tieng Reservoir is located in the tropical monsoon climate. The rainy season is from May to November. The dry season is from December to April. Considering the time of simulation, WQ was divided into two periods: WQ simulation results on January 6, 2019, and March 2, 2019, represented WQ at the beginning and end of the dry season; October 28, 2019, simulated for WQ in the rainy season of Dau Tieng reservoir. Based on the simulation results of the WQ indicators and the WQI index at 3 times in 2019, as shown in Figures 2 and 3, it pointed out that the water source in the dry season was more polluted than in the rainy season. On January 6, 2019, the reservoir water showed signs of pollution, mainly at discharge points (VT3 and VT5), the upstream area of the Tha La stream, and a point below the tributary of the Saigon River. More severe water pollution occurred on March 2, 2019. Almost half of the reservoir area in Tay Ninh province had a WQ of 5-Very Poor level (shown in red). This area had production activities of noodle factories, rubber factories, large-scale pig farms, and agricultural activities (cassava cultivation) in the semi-flooded area of the Dau Tieng reservoir. In this situation, if the authorities do not strictly manage the wastewater treatment before discharging into the Dau Tieng reservoir, as well as the activities of spraying pesticides and using chemical fertilizers in agricultural cultivation, the water in the reservoir will be seriously polluted (DT-PH IEIC, 2019). In the rainy season (image on October 28, 2019), signs of pollution were less detected due to the large volume of water (rainfall in October is more than 300mm). However, in the upstream area of Tha La stream, there was a sign of heavily polluted water because it received water from three streams, including Ta Ly, Ta On, and Ngo. These streams received wastewater from noodle and rubber factories, and in this area, sand mining was quite strong, leading to heavily polluted water sources (DT-PH IEIC, 2019).

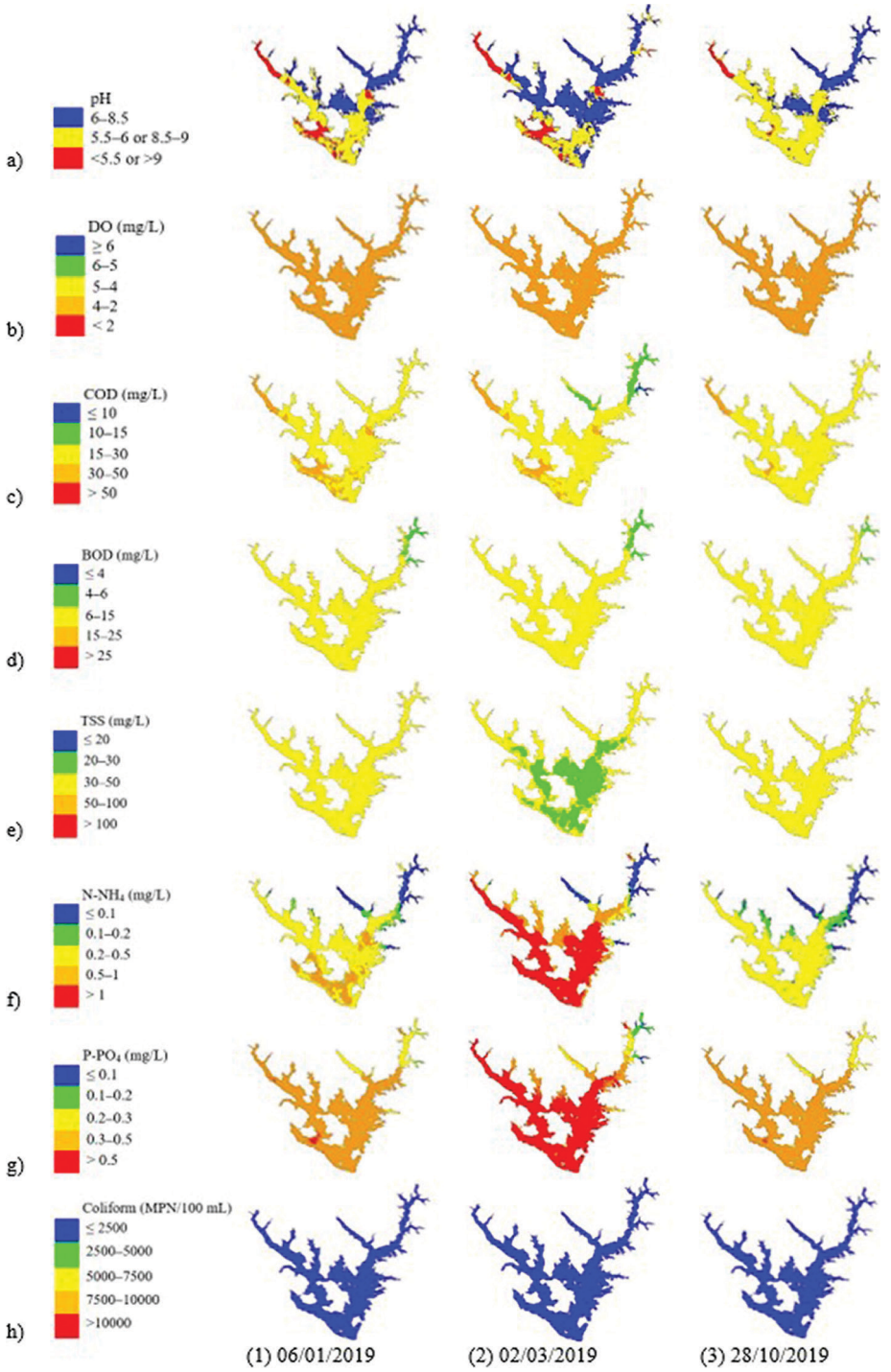

Figure 2: Simulation of concentrations of (a) pH, (b) DO, (c) COD, (d) BOD, (e) TSS, (f) N-NH4, (g) P-PO4, and (h) Coliform at 3 times of image acquisition in 2019

Based on the results of the WQ assessment, it can be seen that, at the time of the study, the water source of the Dau Tieng reservoir was heavily polluted. To improve and protect the WQ of the Dau Tieng reservoir, as well as manage and use water resources appropriately, there should be synchronous coordination between state and reservoir management agencies to have effective management solutions. State agencies must control discharge sources and manage sand mining activities on the reservoir, businesses, and people's agricultural farming activities in semi-flooded areas. The reservoir management agency must build a network of monitoring and collecting information, improve the level, and combine training on using satellite data to evaluate the reservoir WQ synthesis in time and space. In addition, there should be coordination between functional agencies to protect WQ. Strengthening the inspection and supervision of mineral mining activities and environmental protection is necessary. The State should promote coordination between departments, branches, and levels to implement policies and laws on management, exploitation of mineral resources, and environmental protection in the province. Neighboring provinces need to coordinate the implementation of state management in the field of water resources, mineral resources, and environmental protection in areas bordering administrative boundaries between provinces to ensure the initiative, timeliness, efficiency, and consistency in inspection and examination within the border areas between provinces and cities.

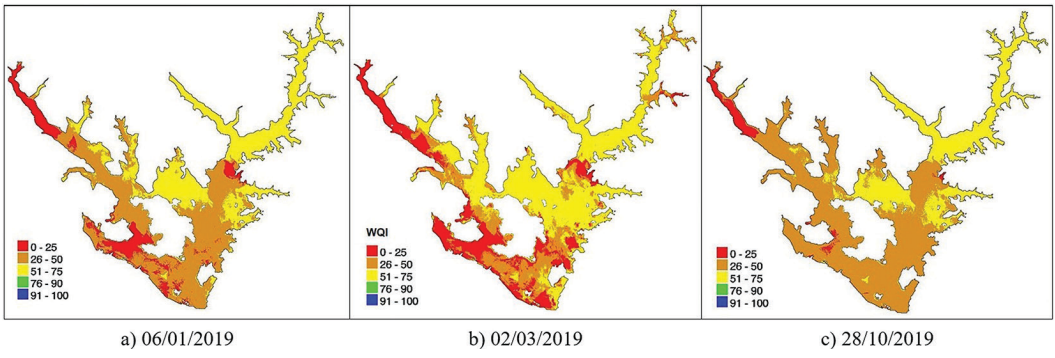

Figure 3: Simulation of WQI index at 03 times of image acquisition in 2019.

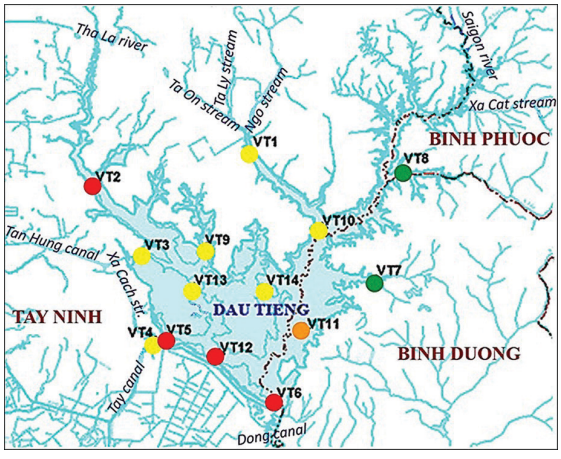

Figure 4: WQI at the location of ground monitoring points on 02/03/2019

4 CONCLUSION

In the results of this study, we calculated WQI at 14 monitoring points on the lake. The study combines ground observation and Sentinel-2A satellite image data with a regression function showing their correlation. The regression functions showed that the correlation of the WQ indicators was associated with single bands, and the band ratio included the blue band and NIR, red/blue, green/blue, and NIR/blue. The results of calculating WQI according to satellite images compared with WQI at 14 monitoring points showed that most pollution levels were similar with 11/14 observation points (about 79%). Only 3 points have a slight deviation of one level. This limitation is related to the image's spatial resolution, which will be improved in our future studies.

The simulation image of the spatial distribution of the WQI demonstrates that the water source of the Dau Tieng reservoir was already in a polluted state, with the WQI ranging from 0 to 50 being the majority. Therefore, appropriate treatment measures should be taken if it needs to be used for domestic water supply purposes. Regarding spatial distribution, WQ in the Dau Tieng reservoir's western, northwest, and southwest areas is heavily polluted. In contrast, in the streams and canals in the eastern and northeastern areas of the reservoir, the WQ has been improved. Water supplies for domestic, industrial, agricultural, irrigation, livestock, and other purposes on the reservoir require constant monitoring to ensure the required standards are applied.

The limitation of our study is that the sample data set is still small. But with this method, the results gave us a better understanding of the study area on the spatial scale of the whole reservoir thanks to the relationship between the ground sample and the satellite-based spectral value. While in practice it is difficult for humans to simultaneously carry out detailed sampling to simulate the distribution over a large space at a time of observation. Remote sensing technology with a wide coverage area, quick update time, and diverse spectrum range can be combined with the WQI calculation method based on monitoring results in water pollution research, bringing an effective solution for environmental managers, especially for river and lake systems. Given the worsening environmental problems in the Dau Tieng reservoir, integrated management approaches of remote sensing and in situ samplings are necessary to protect the lake water quality.

Acknowledgments

This research is funded by Vietnam National University HoChiMinh City (VNU-HCM) under grant number C2021-20-21. We would like to thank Ho Chi Minh City University of Technology (HCMUT), VNU-HCM for the support of time and facilities for this study. The authors are grateful to the United States Geological Survey (USGS), the National Aeronautics and Space Administration (NASA) for accessing the satellite imageries used for this study.

Literature and reference:

Al-Bahrani, H.S., Abdul Razzaq, K.A. & Saleh, S.A.H. (2012). Remote sensing of water quality index for irrigation usability of the Euphrates River. WIT Transactions on Ecology and The Environment, 164, 55-66.

Alparslan, E., Aydöner, C., Tufekci, V., Tufekci, H. (2007). Water quality assessment at Ömerli Dam using remote sensing techniques. Environ Monit Assess 135, 391-398

Canty, M. (2010). Image analysis, classification and Change detection in Remote Sensing. CRC Press.

DT-PH IEIC, Dau Tieng - Phuoc Hoa Irrigation Engineering Integrated Company (2019). Report on inspection and assessment of surface water quality of Dau Tieng reservoir. (in Vietnamese)

Ekstrand, S. (1992). Landsat TM based quantification of chlorophyll-a during algae blooms in coastal waters. International Journal of Remote Sensing, 13(10), 1913-1926.

ESA (2015). Sentinel-2 User Handbook

Fayma, M. & Mili, G.N.L. (2016). Remote estimation of water quality parameters of Himalayan Lake (Kashmir) using Landsat 8 OLI imagery. Geocarto Internatlonal, 32(3), 274-285.

Guan, X. (2009). Monitoring Lake Simcoe Water Quality using Landsat TM Images. Master thesis of Science in Geography, University of Waterloo.

Ha, N.N., Huong, T.T.T, Vinh, P.T. & Van, T.T. (2021). Surface Water Pollution Risk From Vietnam Water Quality Index (VN-WQI) in the Ca Mau City, Mekong Delta. Nature Environment and Pollution Technology, 20(4), 1449-1464.

Ha, N.T.T., Cang, B.D., Thao, N.T.P. & Nhi, B.T. (2016). Experimental modeling of the spatial distribution of chlorophyll-a content and eutrophication index of Ho Tay water using Sentinel-2A images. VNU Science Journal: Earth and Environmental Sciences, 32(2S), 121-130. (in Vietnamese)

Hoang, T. & Ngoc, C.N.M. (2008). Analyze research data with SPSS. Hong Duc Publishing House. (in Vietnamese)

Karakaya, N., Evrendilek, F. (2011). Monitoring and validating spatio-temporal dynamics of biogeochemical properties in Mersin Bay (Turkey) using Landsat ETM+. Environ. Monit. Assess.,181, 457–464

Karaoui, I., Boudhar, A., Abdelkrim, A., Mohammed, H., Mouatassime, S.E, Kamal, A.O., Driss, E., Idrissi, E.A. & Nouaim, W. (2019). Evaluating the potential of Sentinel-2 satellite images for water quality characterization of artificial reservoirs: The Bin El Ouidane Reservoir case study (Morocco)", Meteorology Hydrology and Water Management, 7(1),31–39.

Luu, P.T. (2017). Environmental factors regulating cyanobacterial population in the Dau Tieng reservoir. Journal of Science, Natural Sciences and Technology, Ho Chi Minh City University of Education, 14(12), 107-116

Mateos, C.J.B., Ruiz, C.P., Crespo, R.G. & Sanz, A.C. (2010). Relative Radiometric Normalization of Multitemporal images. International Journal of Artificial Intelligence and Interactive Multimedia, 1(3), 54-59

MONRE, Ministry of Natural Resources and Environment (2015). QCVN 08-MT:2015/BTNMT National technical regulation on surface water quality. Ha Noi, Vietnam. (in Vietnamese)

My, N.T. (2019). Analysis of water quality in Dau Tieng reservoir by remote sensing method. Master thesis of Environment, HCMC University of Technology, VNU-HCM.

O'Reilly, J.E., Maritorena, S.B., Mitchell, B.G., Siegel, D.A., Carder, K.L., Garver, S.A., Kahru, M., & McClain, C. (1998). Ocean color chlorophyll algorithms for SeaWiFS. Journal of Geophysical Research, 103(C11), 937-953.

Park, Y-J., & Ruddick, K. (2007). Detecting algae blooms in European waters. Envisat Symposium 2007, ESA SP-636.

Phi, N.Q., Nhu, N.T.H., Manh, N.D., Cuong, L.P., Huy, L.V., Hoang, L.H. & Nguyet, N.T.A. (2014). Research and assessment of surface water quality in the coastal area of the bottom mouth using remote sensing technology. Proceedings of the National GIS application conference. (in Vietnamese)

Prosper, B., Elhadi, A., Mohamed, A.M.A.E. & Samuel, A. (2018). Comparing Landsat 8 and Sentinel-2 in mapping water quality at Vaal Dam. Proceedings of International Geoscience and Remote Sensing Symposium (IGARSS 2018), 9280-9283.

Phuong, N.T.B., Tri, V.P.D., Du, N.B., & Nguyem, N.C. (2017). Remote Sensing for Monitoring Surface Water Quality in the Vietnamese Mekong Delta: The Application for Estimating Chemical Oxygen Demand in River Reaches in Binh Dai, Ben Tre. Vietnam Journal of Earth Sciences, 39(3), 256-269.

Ritchie, J.C., Zimba, P.V. & Everitt, J.H. (2003). Remote sensing techniques to assess water quality. Photogrammetric Engineering & Remote Sensing, 69, 695.

Sakuno, Y., Maeda, A., Mori, A., Ono, S., Ito, A. (2019). A Simple Red Tide Monitoring Method using Sentinel-2 Data for Sustainable Management of Brackish Lake Koyama-ike, Japan. Water, 11, 1044

The Nhan & Hong Tham (2020). Improve water quality of Dau Tieng Reservoir-Needs synchronous solutions. https://baotayninh.vn/can-cac-giai-phap-dong-bo-a123429.html

Trung, L.V. (2015). Remote sensing book. Publisher of Vietnam National University in Ho Chi Minh City.

Van, T.T., Bao, H.D.X., My, P.T.A., Phong, T.L., Tri, T.V. (2017). Simulation of river water quality from in-situ data and satellite imagery focuses on organic pollutants. Proceedings of the 2nd International Electronic Conference on Water Sciences (ECWS-2) on 16–30 November 2017

VEA, Vietnam Environment Administration (2011). Decision 879/QD-TCMT on Manual for calculating WQ index from environmental monitoring data of continental surface water. Ha Noi, Vietnam. (in Vietnamese)

Vermote, E., Tanre, D., Deuz, J. & Herman, M., Morcette, J.-J. (1997). Second simulation of the satellite Signal in the Solar Spectrum, 6S: an overview. IEEE Transactions Geoscience and Remote Sensing, 35(3), 675-686.

WHO (2011). Guidelines for Drinking-water Quality. Fourth Edition

Van T.T., Bao H.D.X, My N.T., Thong N.H., Phuong D.T.K., Truong N.N., Duong P.T., Trinh H.B.V. ((2023). Assessment of Dau Tieng reservoir water quality using standard criteria combined with remotely sensed images.
Geodetski vestnik, 67 (3), 343-362.
DOI: https://doi.org/10.15292/geodetski-vestnik.2023.03.343-362

Assoc. Prof. Van Tran Thi
Ho Chi Minh City University of Technology, (HCMUT), 268 Ly Thuong Kiet Street, District 10, Ho Chi Minh City, Vietnam
Vietnam National University Ho Chi Minh City (VNU-HCM), Linh Trung Ward, Thu Duc District, Ho Chi Minh City, Vietnam
e-mail: tranthivankt@hcmut.edu.vn

Dr. Bao Ha Duong Xuan
Ho Chi Minh City University of Technology, (HCMUT), 268 Ly Thuong Kiet Street, District 10, Ho Chi Minh City, Vietnam
Vietnam National University Ho Chi Minh City (VNU-HCM), Linh Trung Ward, Thu Duc District, Ho Chi Minh City, Vietnam
e-mail: baohdx@hcmut.edu.vn

Msc. My Nguyen Thi
Ho Chi Minh City University of Technology, (HCMUT), 268 Ly Thuong Kiet Street, District 10, Ho Chi Minh City, Vietnam
Vietnam National University Ho Chi Minh City (VNU-HCM), Linh Trung Ward, Thu Duc District, Ho Chi Minh City, Vietnam
e-mail: mynguyen10493@gmail.com

BE. Thong Nguyen Hoang
Ho Chi Minh City University of Technology, (HCMUT), 268 Ly Thuong Kiet Street, District 10, Ho Chi Minh City, Vietnam
Vietnam National University Ho Chi Minh City (VNU-HCM), Linh Trung Ward, Thu Duc District, Ho Chi Minh City, Vietnam
e-mail: 2171063@hcmut.edu.vn

Msc. Phuong Dinh Thi Kim
Ho Chi Minh City University of Technology, (HCMUT), 268 Ly Thuong Kiet Street, District 10, Ho Chi Minh City, Vietnam
Vietnam National University Ho Chi Minh City (VNU-HCM), Linh Trung Ward, Thu Duc District, Ho Chi Minh City, Vietnam
e-mail: dtkphuong@hcmut.edu.vn

Msc. Truong Nguyen Nhut
Ho Chi Minh City University of Technology, (HCMUT), 268 Ly Thuong Kiet Street, District 10, Ho Chi Minh City, Vietnam
Vietnam National University Ho Chi Minh City (VNU-HCM), Linh Trung Ward, Thu Duc District, Ho Chi Minh City, Vietnam
e-mail: nhuttruong193@gmail.com

BE. Duong Pham Thuy
Ho Chi Minh City University of Technology, (HCMUT), 268 Ly Thuong Kiet Street, District 10, Ho Chi Minh City, Vietnam
Vietnam National University Ho Chi Minh City (VNU-HCM), Linh Trung Ward, Thu Duc District, Ho Chi Minh City, Vietnam
e-mail: ptduong.sdh221@hcmut.edu.vn

BA. Trinh Ha Bao Van
International University (HCMIU), Linh Trung Ward, Thu Duc District, Ho Chi Minh City, Vietnam
Vietnam National University Ho Chi Minh City (VNU-HCM), Linh Trung Ward, Thu Duc District, Ho Chi Minh City, Vietnam
e-mail: hbvt1800@gmail.com